FK127942 - MOLECULAR PATHOMECHANISM OF SPINK1 MUTATIONS IN PANCREATITIS

Specific Aim 1. Effect of SPINK1 mutations and environmental risk factors on endoplasmic reticulum stress and cell damage.

Chronic pancreatitis frequently develops on the basis of environmental risk factors and genetic susceptibility. The major environmental risk factors in the disease are alcohol abuse and exposure to cigarette smoke. In many cases, the combination of risk factors are required for disease development [1]. Alcohol induces pancreatitis through ER stress [2]. The detrimental effect of alcohol can be amplified by exposure to cigarette smoke. Several studies indicated that smoking reduces pancreatic fluid secretion, stimulates fibrosis, induces the expression of inflammatory cytokines in the pancreas and accelerates the development of pancreatic exocrine insufficiency in chronic pancreatitis [3]. Nicotine and nicotine-derived nitrosamine ketone, the most studied cigarette smoke constituents, predispose to intracellular retention and premature activation of secretory proteases in pancreatic acinar cells, thereby increasing the risk for pancreatitis [4]. The detrimental effect of other smoke constituents on the pancreas is less known. Acrolein, crotonaldehyde and hydroquinone (HQ) are the most cytotoxic chemicals of the thousands of cigarette smoke constituents [5]. Several publications described that these

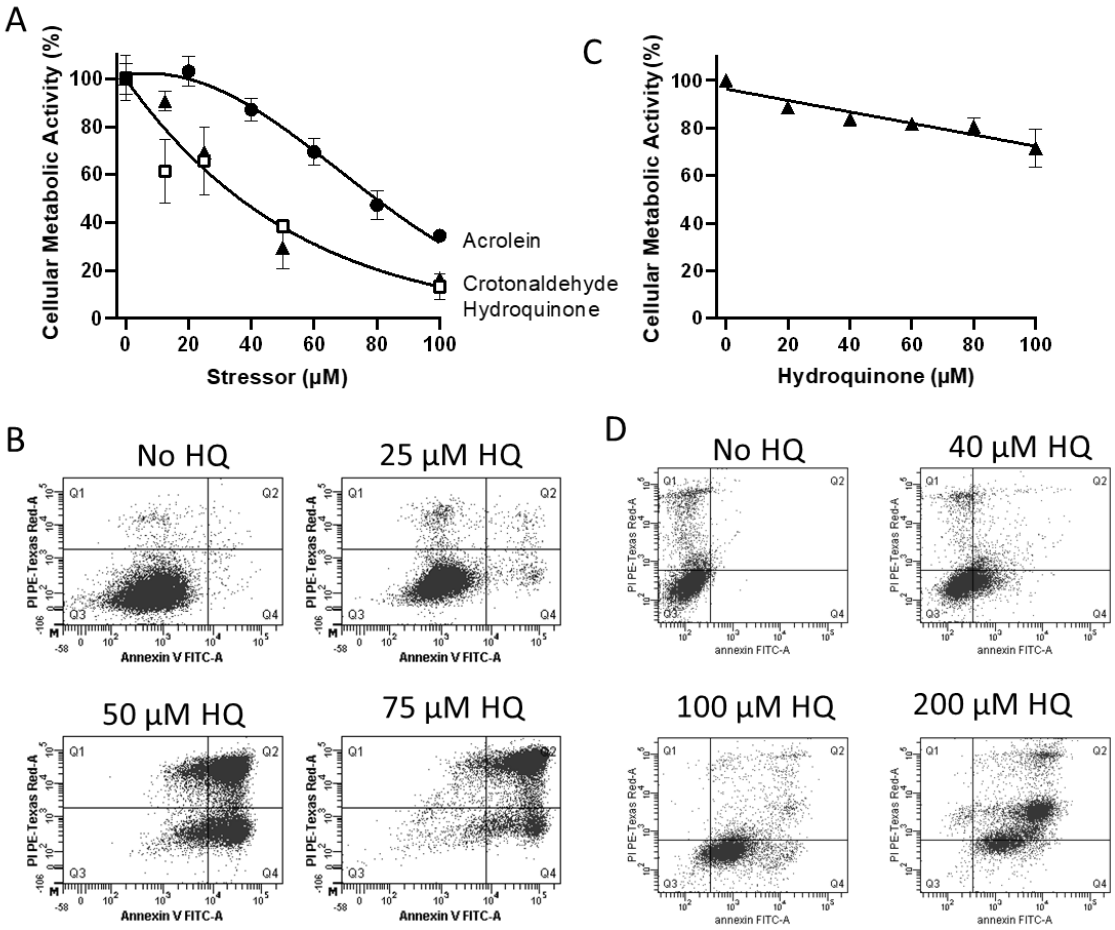

Figure 1. Cytotoxicity of cigarette smoke constituents. A) Viability of HEK 293AD cells in the presence of cigarette smoke toxins. B) FITC-Annexin V / propidium iodide staining of HEK293AD cells in the presence of hydroquinone (HQ). C) Viability of AR42J cells in the presence of HQ. D) FITC-Annexin V / propidium iodide staining of AR42J cells in the presence of HQ.

toxins cause cell death via the activation of ER stress pathways. It has been demonstrated that acrolein upregulates the pro-apoptotic ER stress marker CHOP and induces pancreatic cell death [1]. In addition, HQ diminishes the antioxidant defense system, and activates apoptotic caspases in the pancreas [6]. Following low-dose oral administration, plasma HQ concentrations of 60-70 μM are readily reached in rodents [7]. HQ is a cytotoxic chemical, which can be converted to semiquinone radicals in the cells causing oxidative stress and cell damage [8]. HQ can result in chromosomal aberrations such as mitotic recombination, DNA breaks and chromosomal translocations [9]. In addition, HQ may inhibit the activity of proteasome, and induce ER stress and the formation of autophagosomes [10].

Subaim 1. In this project first we studied the effects of acrolein, crotonaldehyde and HQ on the viability of mammalian cell lines such as HEK 293AD (Figure 1A). Viability was followed with MTT assay by measuring the cellular metabolic activity of the cells. The results showed that acrolein up to 20 μM did not influence cell viability, whereas at higher concentrations, a gradual decrease of viability was observed. Crotonaldehyde and HQ had more detrimental effects on viability, as even at low concentrations both toxins substantially reduced the cellular metabolic activity of HEK 293AD cells. Due to its favorable shelf life and strong effects, we studied the cellular effects of HQ in detail in our further experiments. In order to determine whether decreased cellular metabolism is due to programmed cell death or necrosis, we monitored the amount of FITC annexin V and propidium iodide stained HEK 293AD cells with flow cytometry in the presence of increasing concentrations of HQ (Figure 1B). HQ up to 25 μM did not cause substantial cell death, whereas at 50 and 75 μM HQ programmed cell death occurred, as evidenced by increased staining both with FITC annexin V and propidium iodide. The effect of HQ on the viability of differentiated AR42J pancreatic cells was also tested. We incubated AR42J cells in the presence of increasing concentrations of HQ, and followed viability by measuring metabolic activity with MTT assay (Figure 1C). We found that increasing HQ concentrations up to 100 μM only slightly decreased the viability of AR42J cells. The results suggest that AR42J cells are more resilient to the toxin than the other tested cell line. To test whether programmed cell death

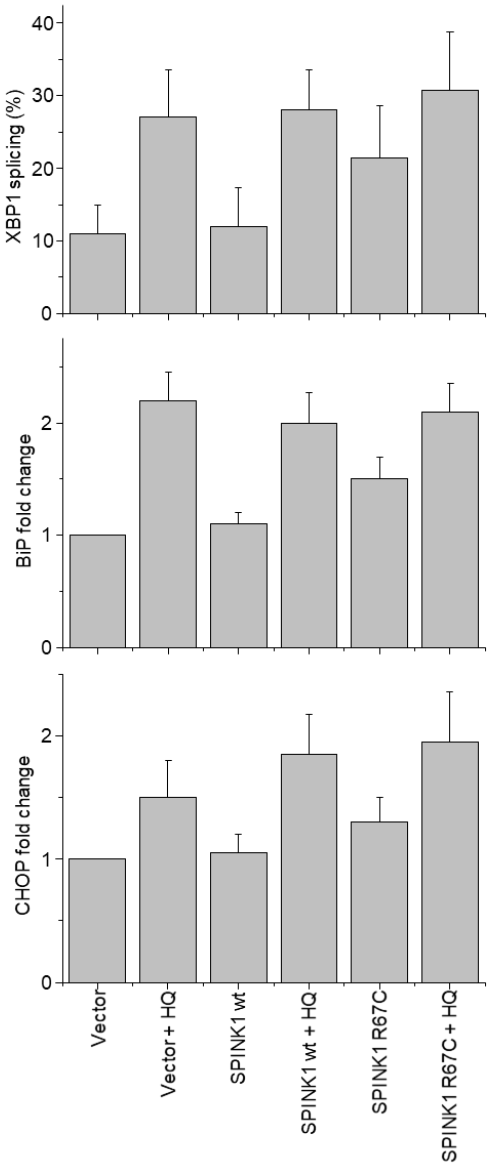

Figure 2. Effect of hydroquinone (HQ) on the levels of ER stress markers in wild-type and SPINK1 R67C expressing HEK 293AD cells. One day post-transfection, cells were incubated in the absence or presence of 25 μM HQ for 24 h at 37 ˚C. The mRNA levels of XBP1 splicing, BiP and CHOP expressions were assessed.

of AR42J also occurs in the presence of HQ, we measured the FITC annexin V and propidium iodide staining of the cells (Figure 1D). Up to 40 μM HQ most of the cells remained unstained by the reagents. The majority of the cells first became annexin V positive in the presence of 100 μM HQ, and also reacted with propidium iodide at an even higher HQ concentration. We hypothesized that cigarette smoke toxins cause endoplasmic reticulum (ER) stress and that is the reason why we observed reduced viability of the cells. To confirm this notion, we monitored the levels of ER stress markers (X-box binding protein, XBP1; Immunoglobulin binding protein, BiP; C/EBP homologous protein, CHOP) of the unfolded protein response pathways. We found that HQ induces ER stress in both cell lines, demonstrated by elevated levels of XBP1 mRNA splicing, and increased expression of BiP and CHOP (Figures 2 and 3). We also studied the effect of ethanol at the physiologically relevant 50 mM concentration. In contrast with the cigarette smoke components, ethanol had only a slight negative effect on cell viability without the induction of endoplasmic reticulum stress (not shown).

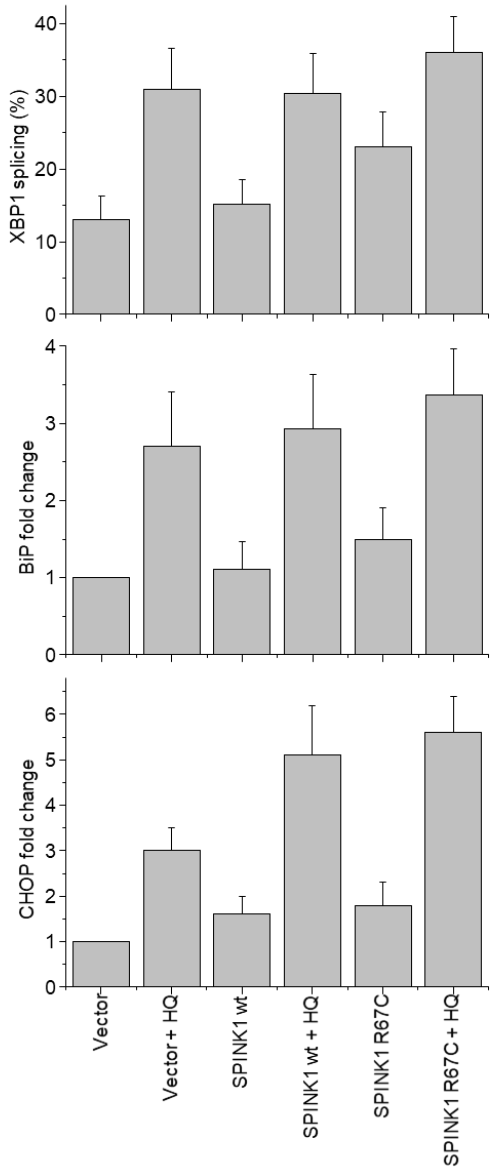

Figure 3. Effect of hydroquinone (HQ) on the levels of ER stress markers in wild-type and SPINK1 R67C expressing AR42J cells. One day post-transfection, cells were incubated in the absence or presence of 25 μM HQ for 24 h at 37 ˚C. The mRNA levels of XBP1 splicing BiP and CHOP and NQO1 expressions were assessed.

We hypothesized that cigarette smoke may increase the severity of pancreatitis caused by genetic determinants. Therefore, we cultured and transfected HEK 293AD cells with plasmid DNA carrying the coding sequence of SPINK1 R67C mutant and wild type as a control. After 15h incubation the cells were rinsed with Opti-MEM and treated with 25 μM hydroquinone. After 24 h incubation the cells were subjected to viability test with MTT assay. In contrast with wild-type SPINK1, the mutant inhibitor decreased cell viability by 20% (Figure 4). The addition of hydroquinone further decreased the viability by about 10%. The results indicated that cigarette smoke components may increase the toxic effect of genetic susceptibility. We also isolated RNA from the cells and after reverse transcription we measured the levels of ER stress markers. We found slightly increased levels of ER stress markers in cells expressing SPINK1 R67C, while the addition of the cigarette smoke component hydroquinone to the transfected cells had only a minor additional impact on ER stress (Figure 2).

AR42J cells cannot be transfected efficiently with plasmid DNA. Therefore, we developed lentiviral and adenoviral vectors and compared their efficiency in gene transfer.

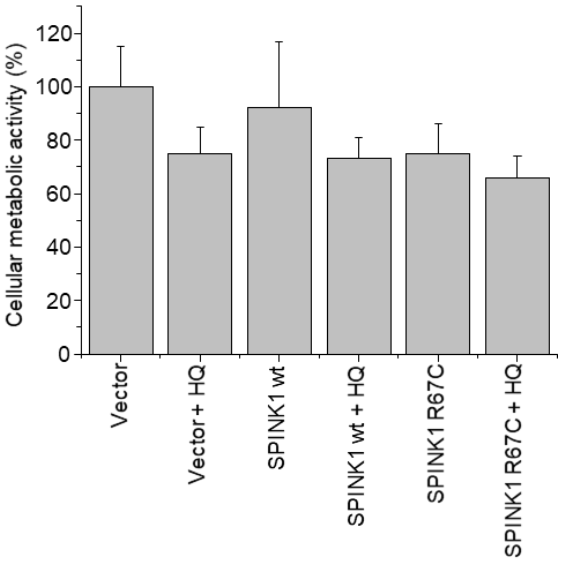

Figure 4. Viability of SPINK1 wild-type and R67C mutant expressing HEK 293AD cells in the presence and absence of hydroquinone (HQ). Viability was determined 24 h after transfection by measuring cell metabolic activity with MTT assay.

Development of lentiviral vectors

Lentiviral vector pTy was readily available in the Laboratory of Retroviral Biochemistry, Department of Biochemistry and Molecular Biology at the University of Debrecen. Therefore, we cloned the SPINK1 coding sequence which carries the first intron of SPINK1 gene into the pTy lentiviral vector using the restriction sites SalI and KpnI. As a consequence, the cDNA of GFP protein was removed and replaced by SPINK1 cDNA. Empty pTy vector was also generated by the removal of the GFP cDNA. To test whether the SPINK1-pTy plasmid is functional, we cultured HEK 293T cells in a 6-well-plate in DMEM medium supplemented with 10% FBS and 2 mM Gln; and transfected the cells at a confluence of 80-90% with the plasmid DNA and PEI transfection reagent. On the next day, cells were rinsed with Opti-MEM and fresh Opti-MEM was added to the wells. After 48 h incubation the media were harvested and subjected to trypsin inhibition experiments. 10 nM trypsin was mixed with 0.05 mL medium in 0.1 mL final volume. After 20 min incubation, 0.150 mM Suc-AAPK-pNA substrate was added, and the residual trypsin activity was followed with a plate reader at 405 nm. Medium from cells transfected with empty pTy served as a control. We found full inhibition in assays with media containing SPINK1 protein in contrast to the negative controls where 60 mOD/min trypsin activities were detected. These results indicated that our SPINK1-pTy vector is functional. To produce lentiviral particles carrying our SPINK1 construct we seeded HEK 293T cells into T75 cell culture flasks. At 80% confluence, we cotransfected HEK 293T cells with the SPINK1-pTy, psPAX2 and pMDG plasmids using polyethyleneimine transfection reagent in DMEM/1% FBS/2 mM Gln. The psPAX2 and pMDG vectors are responsible for the expression of viral structural proteins and packaging of the virus. After 5-6 h incubation the medium was discarded and fresh DMEM supplemented with 10% FBS was added to the flasks. The medium was harvested after 48h and lentiviral particles were isolated with ultracentrifugation at 100000 g for 2 hours. The supernatant was discarded and the pellet was suspended in 0.2 mL PBS. The retroviral propagation was tested using the Colorimetric reverse transcriptase assay (Roche). The test reported 150-330 ng/mL reverse transcriptase amount, which corresponds to ~10^9 virions/mL.

Development of adenoviral vectors

Alternatively, we developed an adenoviral vectors to deliver SPINK1 and study the effect of SPINK1 mutations on secretion of the inhibitor in AR42J rat acinar cells. To perform expression studies, SPINK1 coding DNA carrying the first intron was cloned into the pO6A5 shuttle vector (Sirion Biotech) using the restriction sites NheI and KpnI. The pO6A5-SPINK1

positive clones were verified after transformation of PIR1 competent cells (ThermoFisher Scientific). The expression of SPINK1 was tested after transfection of HEK 293T cells using the protocol described above. E. coli BA5-FRT competent cells (Sirion Biotech) were transformed with the shuttle vector in which the vector was recombined into the endogenous SIR-BAC-Ad5 adenoviral BAC vector. The recombinant BAC vector was isolated from the cells and purified. The BAC DNA was linearized by cleavages at the PacI restriction sites and analyzed on a 0.8% agarose gel. HEK 293AD cells were cultured on a 6-well-plate in DMEM supplemented with 10% FBS and transfected with the linearized BAC DNA and PEI transfection reagent. After three days incubation the cells were harvested, washed with DMEM supplemented with 10% FBS and lysed with freeze-thaw cycles. The isolated adenovirus was amplified in two additional cycles in HEK 293AD cells using T75 tissue culture flasks. The amplified virions were isolated with freeze-thaw cycles and purified using the AdenoONE Purification Kit (Sirion Biotech). The concentration of functional viral particles was determined with AdEasy viral titer kit (Agilent). Typical virus concentration in our purified samples was 10^7 to 10^9 infectious unit per mL, which is suitable for transduction experiments.

We infected differentiated AR42J cells with increasing concentrations of lentivirus and adenovirus carrying SPINK1. The results showed that adenoviral vectors are more efficient in gene delivery to AR42J than lentiviral vectors (not shown). Therefore, in our further experiments we used adenoviruses carrying His-tagged SPINK1 wild type and R67C coding DNA. Earlier preliminary data indicated that the R67C mutation causes secretion defect of SPINK1 and induces a slight but consistent endoplasmic reticulum (ER) stress. AR42J cells were cultured onto 12-well tissue culture plates (using 0.4 million cells/well) in DMEM medium supplemented with 20% FBS, penicillin/streptomycin antibiotics and 100 nM dexamethasone. After 48h incubation in a standard tissue culture incubator, the culture media were removed and the cells were rinsed with OptiMEM reduced serum medium. Fresh OptiMEM was added into each well, and the acinar cells were transduced by the addition of wild-type and mutant SPINK1 carrying adenoviruses in a concentration of 10^8 particles/ml determined by AdEasy viral titer kit. As a negative control adenovirus without SPINK1 DNA was used. Note that adenovirus at higher concentration caused cell death, whereas at lower concentrations the cells did not produce SPINK1. After an additional 48 h incubation the conditioned media were harvested and the acinar cells were lysed, and proteins and RNA were isolated. The secretion of SPINK1 in AR42J was followed by trypsin inhibition assays or SDS-PAGE and western blotting (not shown). In agreement with our previous experiments using HEK cells, we found that SPINK1 wild type was readily secreted into the conditioned medium of AR42J, whereas the R67C protein could not be detected. Analysis of cell lysates indicated that variant R67C retained inside the cell probably due to protein misfolding.

In order to study the cellular effects of SPINK1 mutation on AR42J, RNA from cell lysates were purified and reverse transcribed. The level of ER stress markers XBP1 messenger splicing and BiP and CHOP expression in cells producing SPINK1 wild type and R67C were determined with PCR techniques (Figure 3). XBP1 protein, synthesized from the spliced messenger, is a transcription factor responsible for the production of ER resident proteins to resolve ER stress, while BiP is a chaperone located in the ER. We found that similarly to the effect of control adenovirus, cells infected by SPINK1 wild type adenovirus possessed only 15% XBP1 spicing. A slight but consistent increase was observed after treatment with SPINK1 mutant adenovirus. In agreement with these results, BiP expression was also increased about 1.5-fold in cells treated with SPINK1 mutant adenovirus in contrast with the effect of wild-type and control adenoviruses which did not influence BiP expression. Interestingly, CHOP

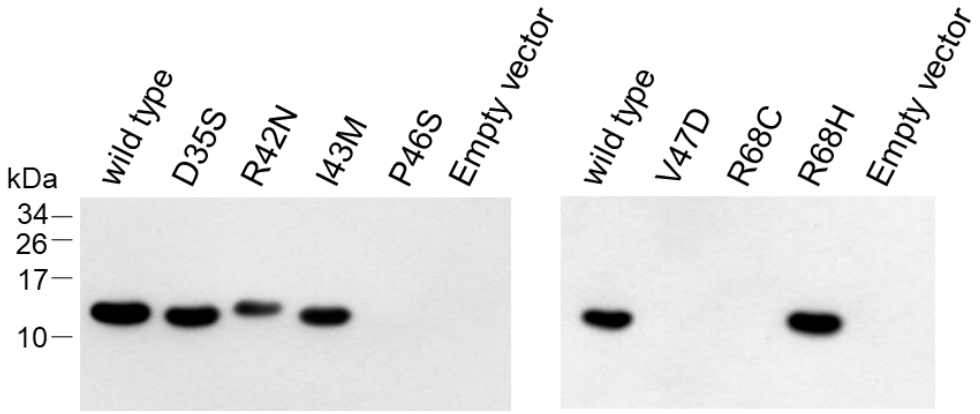

Figure 5. Secretion of Spink3 variants in HEK 293T cells. Conditioned media of transfected cells were analized with SDS-PAGE and immunoblotting. Spink3 wild type and variants D35S, R42N, I43N, R68H were readily secreted, whereas mutants P46S, V47D and R68C retained in the cells.

expression was not substantially induced in mutant SPINK1 expressing cells. The observed mild biological effects suggest that the SPINK1 R67C variant causes pancreatitis through reduced inhibitor secretion rather than through ER stress.

To study the effect of the genetic risk factor in combination with cigarette smoke, we performed MTT cell viability assays and detected the levels of ER stress markers XBP1 messenger splicing and BiP expression in the absence and presence of hydroquinone in SPINK1 wild type and mutant R67C expressing cells (Figure 3). We found that hydroquinone resulted in a slightly stronger ER stress in cells expressing mutant SPINK1 than wild-type SPINK1 indicated by considerably increased BiP and CHOP expressions and XBP1 messenger splicing.

In parallel experiments, we also studied the combined effect of a misfolding pancreatic lipase mutation G233E and the cigarette smoke toxin HQ. In which case we found even larger combined effects of the mutation and toxin. Our major findings were published recently in PLoS One (PLoS One 17(6):e0269936).

Subaim 2. The mouse pancreas also secretes a pancreatic secretory inhibitor protein highly homologous to human SPINK1. The inhibitor protein is called Spink3. First, we studied the effect of eight SPINK1 mutations identified in chronic pancreatitis patients on the secretion of Spink3 (Figure 5). HEK 293 cells were transfected with Spink3 plasmid DNA. Spink3 in the conditioned media were detected with SDS-PAGE. Mutations D35S, R42N, I43M, A56S and R68H did not alter normal Spink3 secretion, whereas mutations P46S, V47D and R68C completely diminished the inhibitor secretion. Note that amino acid numbering of Spink3 is different from SPINK1 due to a one amino acid longer signal peptide. We focused on SPINK1 mutation (R68C in Spink3), which caused a slight but well-detectable decrease in viability in transfected cells (Figure 4). Spink3 wild type and R68C expressing cells were harvested, lysed and RNA was purified. After reverse transcription the levels of ER stress markers XBP1 messenger splicing and BiP expression were assessed with PCR techniques. As a control, cells transfected with empty plasmid DNA were used. We found that the levels of ER stress markers were low in cells producing wild-type Spink3. In contrast, a slightly increased levels (1.3-1.5-fold) of ER stress markers were observed in cells expressing Spink3 mutant (Figure 6). Cell viability was also assessed with MTT assay. In contrast to the wild-type Spink3 producing cells which decreased viability by 15%, the mutant Spink3 expressing cells reduced viability by 40%. To study the effect of cigarette smoke constituents on wild-type Spink3 and mutant R68C

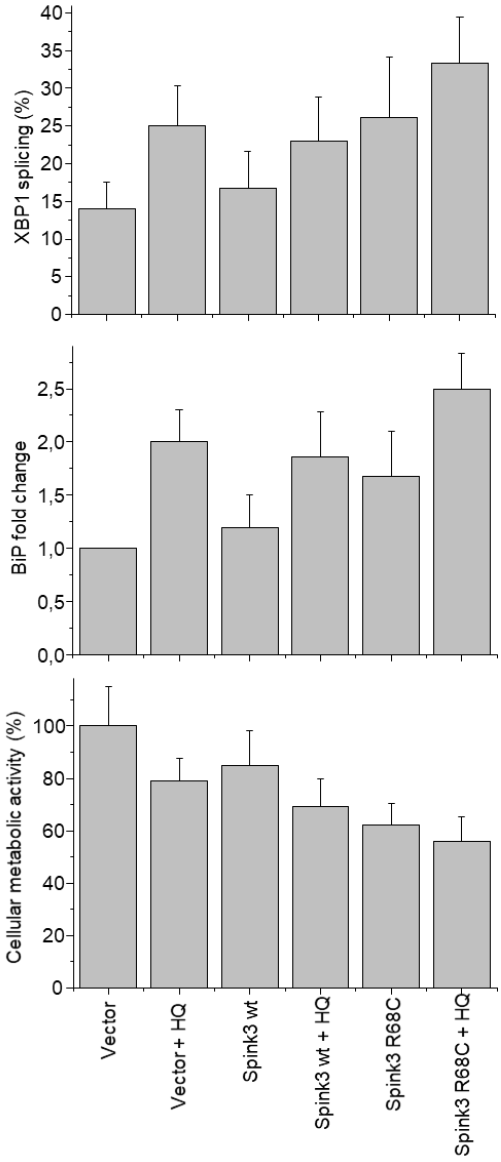

Figure 6. Cellular effects of non-secreted Spink3 variants. ER stress markers XBP1 mRNA splicing and BiP expression were assessed 48 h after transfecting HEK 293AD cells. Viability of HEK 293AD cells were determined with MTT assay.

expressing cells, we incubated transfected cells in the presence or absence of 25 μM hydroquinone. We found that the treatment of mutant Spink3 expressing cells by hydroquinone caused further increased levels of ER stress indicated by considerably elevated BiP expression and XBP1 messenger splicing. Whereas, the levels of ER stress in wild-type Spink3 expressing cells remained lower. MTT viability test indicated that the higher level of ER stress resulted in a reduced cell viability.

Specific Aim 2. Development and characterization of inhibition defective Spink3 variants

Our major objective was to functionally characterize missense SPINK1 inhibitor mutations identified in chronic pancreatitis. We functionally characterized all 22 variants and we identified only 7 inhibitor variants which did not alter dramatically protein secretion. We created two SPINK1 constructs with and without a C-terminal histidine tag. The secretion of these inhibitor variants were studied in transfected HEK 293T cells by analyzing conditioned media with western blotting and by measuring inhibitory activities against trypsin (Figure 7). For these experiments we used SPINK1 constructs with and without histidine tags. SPINK1 in the conditioned media was detected by a monoclonal anti-SPINK1 antibody or by an antibody developed against the histidine tag. When untagged SPINK1 constructs were studied by immunoblotting, secretion of variants K41N and R65Q was somewhat decreased, whereas the secretion of P55S was slightly increased. All other variants were secreted at similar levels as the wild-type inhibitor. Immunoblotting of histidine tagged SPINK1 showed similar banding pattern, with the exception of variant R65Q, which indicated increased secretion. We also determined SPINK1 levels by measuring the trypsin inhibitory activity of the conditioned media (Figure 7C). The measurements correlated well with the previous experiments. The only exception was observed with untagged Q68R variant, which yielded higher than expected concentrations.

Binding of SPINK1 variants to trypsin

Human trypsins are posttranslationally sulfated at Tyr154 residues, which is part of the substrate binding site of trypsin. We expressed and purified sulfated trypsins from transfected HEK 293T cells. Alternatively, sulfated human trypsins were purified from pancreatic juice samples. Non-sulfated trypsins were recombinantly expressed and purified from *E. coli* cells

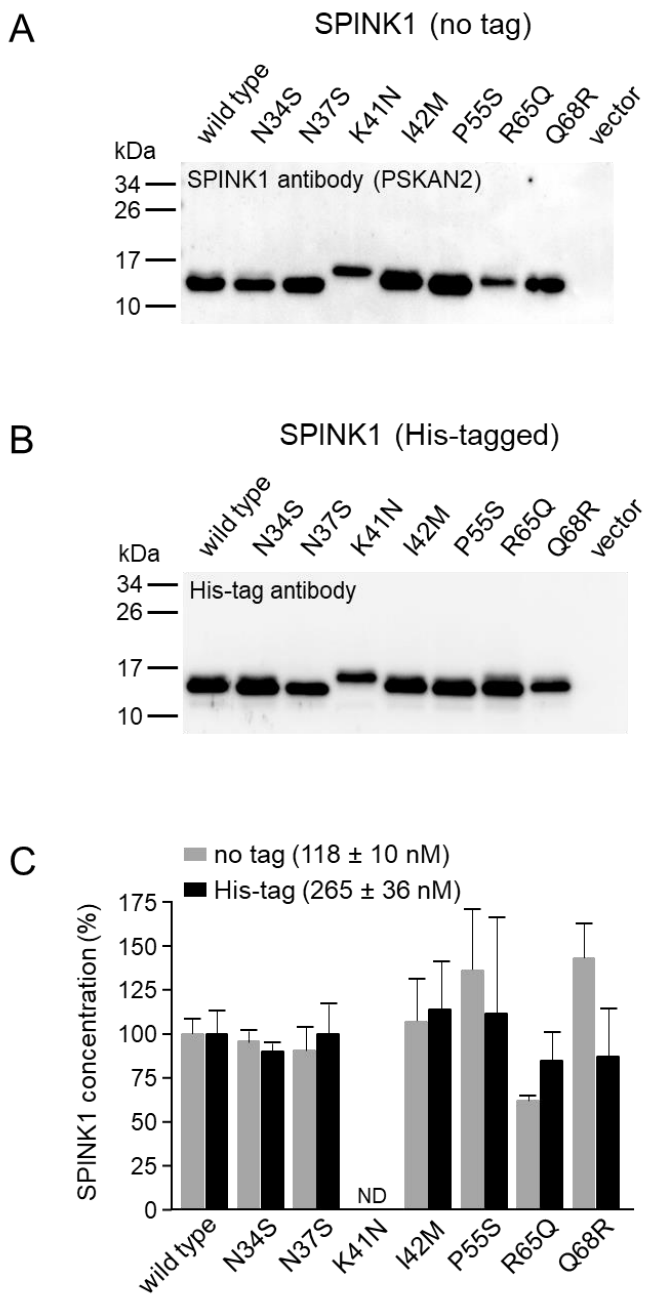

Figure 7. Secretion of SPINK1 variants in HEK 293T cells. Secretion of untagged (A) and tagged (B) SPINK1 wild-type and variants were followed with SDS-PAGE and immunoblotting. Trypsin inhibitory activity (C) of wild-type and mutant SPINK1 was determined with trypsin activity assays.

and sulfation-inhibited HEK 293T cells. We performed equilibrium binding assays (K_D) with wild-type SPINK1 and the frequent N34S variant (Table 1). K_D values were consistently higher against sulfated trypsins versus non-sulfated trypsins. The results indicated that trypsin sulfation weakens SPINK1 binding. When compared with values obtained on trypsins from *E. coli* and pancreatic juice, the K_D values of non-sulfated trypsins from HEK 293T cells were somewhat higher, whereas those of sulfated trypsins from HEK 293T cells were mostly lower. As a result, the negative effect of trypsin sulfation on SPINK1 binding appeared smaller in these experiments.

Binding of missense SPINK1 variants to sulfated human trypsins

In addition to N34S, we purified six other His-tagged SPINK1 variants that preserved secretion. To characterize their inhibitory activity, we measured equilibrium binding to sulfated human cationic and anionic trypsins purified from pancreatic juice (Figure 8). Mutant K41N bound poorly to trypsins with micromolar K_D values, that corresponded to a 20000 to 30000-fold reduction in affinity. The reactive site mutant I42M reduced binding by 3 to 7-fold. Mutation P55S caused a slight decrease in binding, by 1.6- to 3.4-fold, which was almost within experimental error. SPINK1 variants N34S, N37S, R65Q and Q68R exhibited K_D values that were similar to or smaller than those of wild-type SPINK1. Taken together, only rare SPINK1 reactive loop variants K41N and I42M that directly affect the reactive-site peptide bond compromised inhibitor binding to a significant extent.

Effect of SPINK1 mutations on mouse Spink3 secretion

To studied the effect of secreted Spink3 variants on the inhibition of mouse trypsin isoforms we used recombinantly expressed and purified proteins. Mice have 20 trypsinogen genes located on chromosome 6, but only four trypsinogen isoforms (7, 8, 9 and 20) are expressed in large quantities by the mouse pancreas. Trypsinogen 7 is the most abundant one

Table 1. SPINK1 wild-type and N34S mutant binding to sulfated and non-sulfated trypsins.

SPINK1 wild type	Hu1 (E. coli)	Hu1-SO_4 (native)	Hu2 (E. coli)	Hu2-SO_4 (native)
k_{on} (x10^6 $M^{-1}s^{-1}$)	3.02 ± 0.25	3.46 ± 0.15	3.80 ± 0.17	2.40 ± 0.12
k_{off} (x10^{-6} s^{-1})	8.18 ± 0.27	54.8 ± 6.19	0.50 ± 0.04	18.1 ± 0.82
K_D (pM)	2.71	15.8	0.13	7.54
$K_{D(eq)}$ (pM)	1.11 ± 0.20	62.2 ± 10.3	0.25 ± 0.02	36.7 ± 2.3

SPINK1 N34S	Hu1 (E. coli)	Hu1-SO_4 (native)	Hu2 (E. coli)	Hu2-SO_4 (native)
k_{on} (x10^6 $M^{-1}s^{-1}$)	5.34 ± 0.23	2.74 ± 0.22	5.12 ± 0.24	3.10 ± 0.25
k_{off} (x10^{-6} s^{-1})	6.97 ± 0.64	45.0 ± 5.1	0.42 ± 0.01	13.6 ± 0.46
K_D (pM)	1.31	16.4	0.08	4.39
$K_{D(eq)}$ (pM)	1.53 ± 0.20	32.3 ± 2.9	0.38 ± 0.13	16.7 ± 0.8

and contributes about 60% of total trypsinogen. Expression plasmid pTrap-T7 carrying mouse trypsinogen 7, 8, 9 and 20 were obtained from the laboratory of Miklos Sahin-Toth (UCLA, USA). Similarly to human trypsinogens we expressed mouse trypsinogens in *E. coli* BL21(DE3) cells. The cells were lysed with ultrasonic cell disruptor and trypsinogen was in vitro refolded. Trypsinogen isoforms were purified with ecotin affinity chromatography and activated by human recombinant enteropeptidase. The concentration of mouse trypsinogen isoforms was determined by active site titration with ecotin inhibitor. The typical concentration of mouse trypsinogen preparations was about 8-12 μM. To increase the yield of Spink3, exon-1 and exons 2-4 were custom synthesized separately and cloned into the human SPINK1 minigene-1 pcDNA3.1(-) plasmid using XhoI/XcmI and EcoRI/HindIII restriction pairs, respectively. The construct also carried a C-terminal histidine-tag for affinity purification. We cultured and transiently transfected HEK 293T cells with wild-type, D35S, R42N, I43M, A56S and R68H Spink3

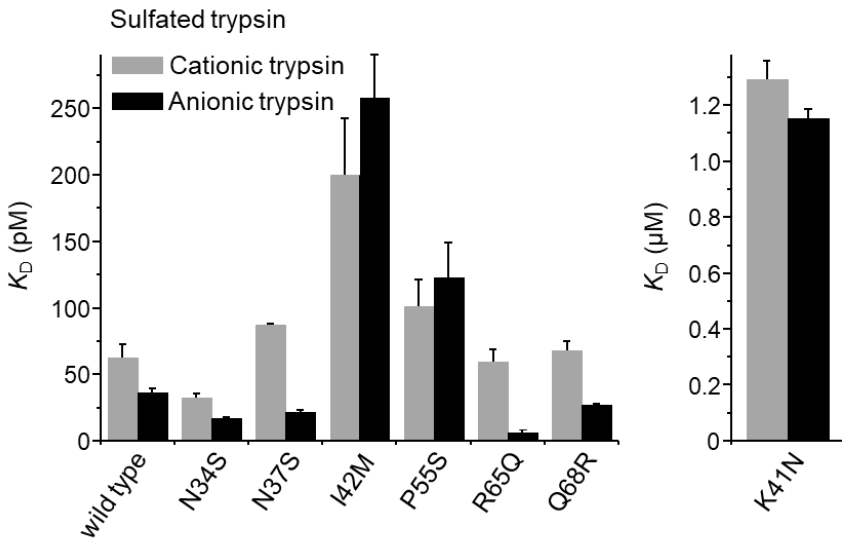

Figure 8. Equilibrium dissociation constants of wild-type SPINK1 and seven variants with sulfated human trypsins.

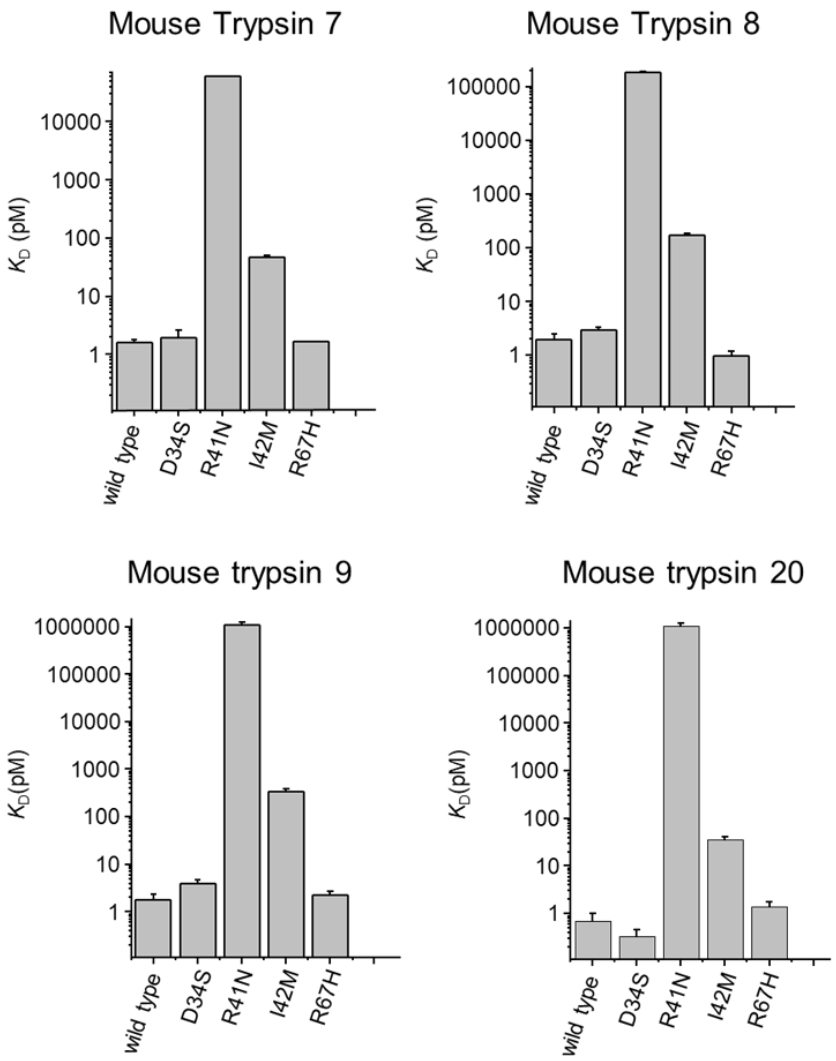

Figure 9. Binding of Spink3 variants to mouse trypsin isoforms.

minigene-1 plasmid DNAs in T75 tissue culture flasks. Spink3 proteins were purified with nickel affinity chromatography. The concentration of Spink3 wild-type and variants were determined with titration against the mouse trypsin isoforms.

First, we determined the equilibrium dissociation constant (K_D) values of Spink3 wild-type and variants against the most abundant trypsin 7 (Figure 9). The wild-type Spink3 inhibited trypsin 7 with a K_D value of 1.8 pM. Consistent with human SPINK1 binding to human cationic trypsin, our data indicated strong inhibitory activity of Spink3 assayed against the mouse trypsin. Mutations D35S, A56S and R68H located in the inhibitor scaffold did not alter K_D value of Spink3 to trypsin 7. In contrast, mutations R42N and I43M increased K_D value by more than 10^4-fold and 10-fold, respectively. Our observations demonstrated that reactive loop mutations decreased the inhibitory function of Spink3. To extend our studies the K_D values of Spink3 wild-type and mutants were also determined against mouse trypsins 8, 9 and 20. Consistent with the previous results, mutations D35S, A56S and R68H did not have an impact on the inhibitory activity of Spink3 assayed with the less abundant mouse trypsin isoforms. Whereas, mutations R42N and I43M increased Spink3 K_D values against trypsins 8, 9 and 20. To confirm our results, we also measured the association and dissociation rate constant values

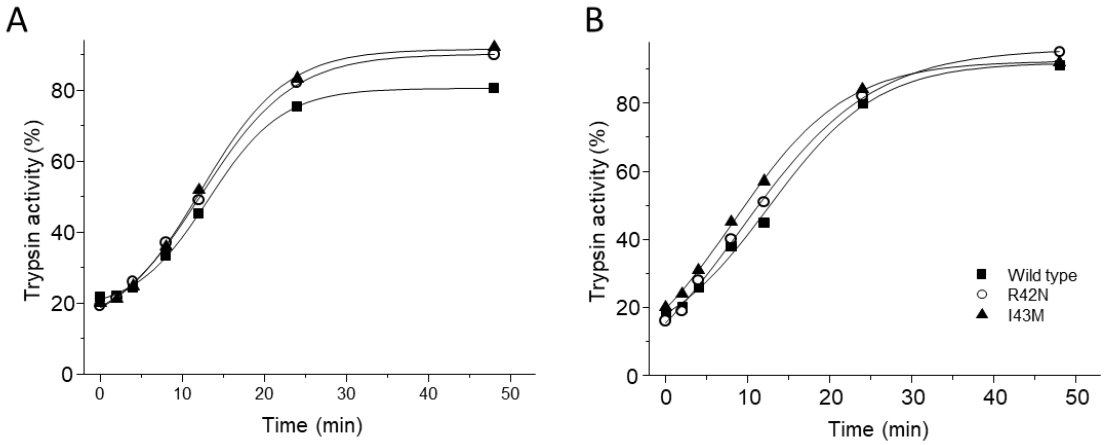

Figure 10. Temporary inhibition of mouse trypsin 7 by wild-type trypsin and variants R42N and I43M. Spink3 at 25 nM was incubated with 30 nM trypsin with (A) and without (B) chymotrypsin C. At given time points aliquotes were withdrawn and trypsin activity was measured.

of Spink3 wild-type and I43M to mouse trypsin 7. We found that the mutation did not alter the association rate but increased the dissociation rate constant by an order of magnitude. We also attempted to measure the kinetic rate constant values for R42N variant, but we could not perform those experiments due to the very weak inhibitory activity of the variant.

SPINK1 is a so-called temporary inhibitor of human trypsin isoforms, as it becomes inactivated over time and digested off by the inhibited proteases. We tested Spink3 degradation by trypsin in the absence and presence of a minor chymotrypsin isoform (chymotrypsin C) which possesses wide substrate specificity (Figure 10). We developed a method to efficiently measure Spink3 degradation in the presence of trypsin and chymotrypsin C. We assayed Spink3 with trypsin in about 1 to 1 ratio in the absence and presence of chymotrypsin C in 10 mM calcium containing buffer to allow Spink3-trypsin complex formation. Calcium at this concentration prevented trypsin cleavage by chymotrypsin C. To measure the levels of intact Spink3, aliquotes were withdrawn and free trypsin levels were detemined by measuring trypsin activities. We found that trypsin slowly degraded wild-type Spink3 and increased free trypsin levels were detected. Mutations R42N and I43M did not influenced trypsin degradation. We repeated the experiment in the presence of chymotrypsin C, which did not affected Spink3 degradation by trypsin. The above described experiments were confirmed with SDS-PAGE and immunoblotting (not shown).

Our preliminary experiments indicated that K41N and I42M reactive loop human SPINK1 variants inhibited human cationic and anionic trypsins with lower affinity than other variants carrying mutations in the inhibitor scaffold. Our data suggested that reactive loop variants may increase the susceptibility for chronic pancreatitis through impaired protease inhibition. Taken together, our results demonstrated that SPINK1 reactive loop variants may increase the susceptibility for chronic pancreatitis. More detailed information on the pathogenicity of mutations could be obtained by developing Spink3 knock-in mouse models.

Based on the results of SPINK1 project, we published three peer-reviewed articles and presented the data at national and international conferences such as the Hungarian Molecular Life Sciences 2021 Conference and the Annual Conference of the European Pancreatic Club. We also published an article about the cellular effects of human pancreatic lipase mutations.

References

1. Lugea A, Gerloff A, Su HY, Xu Z, Go A, Hu C, French SW, Wilson JS, Apte MV, Waldron RT, Pandol SJ. The Combination of Alcohol and Cigarette Smoke Induces Endoplasmic Reticulum Stress and Cell Death in Pancreatic Acinar Cells. Gastroenterology. 2017 Dec;153(6):1674-1686. doi: 10.1053/j.gastro.2017.08.036. Epub 2017 Aug 25. PMID: 28847752; PMCID: PMC5705421.

2. Orekhova A, Geisz A, Sahin-Tóth M. Ethanol feeding accelerates pancreatitis progression in CPA1 N256K mutant mice. Am J Physiol Gastrointest Liver Physiol. 2020 Apr 1;318(4):G694-G704. doi: 10.1152/ajpgi.00007.2020. Epub 2020 Mar 2. PMID: 32116022; PMCID: PMC7191466.

3. Ru N, Xu XN, Cao Y, Zhu JH, Hu LH, Wu SY, Qian YY, Pan J, Zou WB, Li ZS, Liao Z. The Impacts of Genetic and Environmental Factors on the Progression of Chronic Pancreatitis. Clin Gastroenterol Hepatol. 2022 Jun;20(6):e1378-e1387. doi: 10.1016/j.cgh.2021.08.033. Epub 2021 Aug 28. PMID: 34461303.

4. Barreto SG. How does cigarette smoking cause acute pancreatitis? Pancreatology. 2016 Mar-Apr;16(2):157-63. doi: 10.1016/j.pan.2015.09.002. Epub 2015 Sep 18. PMID: 26419886.

5. Stabbert R, Dempsey R, Diekmann J, Euchenhofer C, Hagemeister T, Haussmann HJ, Knorr A, Mueller BP, Pospisil P, Reininghaus W, Roemer E, Tewes FJ, Veltel DJ. Studies on the contributions of smoke constituents, individually and in mixtures, in a range of in vitro bioactivity assays. Toxicol In Vitro. 2017 Aug;42:222-246. doi: 10.1016/j.tiv.2017.04.003. Epub 2017 Apr 28. PMID: 28461234.

6. Bahadar H, Maqbool F, Mostafalou S, Baeeri M, Gholami M, Ghafour-Boroujerdi E, Abdollahi M. The molecular mechanisms of liver and islets of Langerhans toxicity by benzene and its metabolite hydroquinone in vivo and in vitro. Toxicol Mech Methods. 2015;25(8):628-36. doi: 10.3109/15376516.2015.1053650. Epub 2015 Jun 9. PMID: 26056850.

7. English JC, Deisinger PJ. Metabolism and disposition of hydroquinone in Fischer 344 rats after oral or dermal administration. Food Chem Toxicol. 2005 Mar;43(3):483-93. doi: 10.1016/j.fct.2004.11.015. PMID: 15680685.

8. Chouchane S, Wooten JB, Tewes FJ, Wittig A, Müller BP, Veltel D, Diekmann J. Involvement of semiquinone radicals in the in vitro cytotoxicity of cigarette mainstream smoke. Chem Res Toxicol. 2006 Dec;19(12):1602-10. doi: 10.1021/tx060162u. PMID: 17173373.

9. Zhu J, Wang H, Yang S, Guo L, Li Z, Wang W, Wang S, Huang W, Wang L, Yang T, Ma Q, Bi Y. Comparison of toxicity of benzene metabolite hydroquinone in hematopoietic stem cells derived from murine embryonic yolk sac and adult bone marrow. PLoS One. 2013 Aug 5;8(8):e71153. doi: 10.1371/journal.pone.0071153. PMID: 23940708; PMCID: PMC3734044.

10. Xiong R, Siegel D, Ross D. Quinone-induced protein handling changes: implications for major protein handling systems in quinone-mediated toxicity. Toxicol Appl Pharmacol. 2014 Oct 15;280(2):285-95. doi: 10.1016/j.taap.2014.08.014. Epub 2014 Aug 22. PMID: 25151970; PMCID: PMC4312139.